In Vitro Hydroxycarbonate Apatite Mineralization of $CaO-SiO_2$ Sol−Gel Glasses with a Three-Dimensionally Ordered Macroporous Structure

Hongwei Yan,[†] Kai Zhang,[‡] Christopher F. Blanford,[†] Lorraine F. Francis,*[,‡] and Andreas Stein*[,†]

Department of Chemistry, 207 Pleasant Street SE, and Department of Chemical Engineering and Materials Science, 421 Washington Avenue SE, University of Minnesota, Minneapolis, Minnesota 55455

Received November 14, 2000. Revised Manuscript Received February 1, 2001

A three-dimensionally ordered macroporous (3DOM) bioactive glass with a composition of 80 mol % SiO_2 and 20 mol % CaO was synthesized by the sol−gel method using poly(methyl methacrylate) (PMMA) colloidal crystal templates. A control sample with a matching composition was prepared by the same process but without PMMA templating. In vitro hydroxycarbonate apatite growth was investigated by soaking the bioactive glass in simulated body fluid (SBF) at body temperature (37 °C) for varying lengths of time. The formation of a hydroxycarbonate apatite layer on the glass was studied by XRD, SEM, TEM, FTIR, and ICP techniques. The effects of the loading amount and the calcination temperature on the in vitro mineralization process were investigated. The 3DOM bioactive glass exhibited faster growth of apatite than the nontemplated control sample, probably because of its more accessible surface.

Introduction

Bioactive glasses and glass-ceramics have been widely investigated since their discovery.[1−6] These bioactive materials form a biologically compatible hydroxycarbonate apatite (HCA) layer at the interface with bone in vivo.[3−5,7,8] This layer allows the glass to form a continuous bond with bone. An HCA layer can also be formed on the surface of bioactive materials when they are soaked in simulated body fluid (SBF),[9] an aqueous solution that has approximately the same ion concentration and pH as human blood plasma. Researchers have correlated in vitro observations of HCA formation with the in vivo bone-bonding ability of bioactive materials.[10,11] Thus the formation rate of HCA in SBF, sometimes referred to as in vitro bioactivity, can be used to predict the behavior of the bioactive material inside the human body. This discovery has greatly accelerated research on bioactive materials.

The first bioactive glass, in the system $Na_2O-CaO-P_2O_5-SiO_2$, was prepared by a melt method.[1] The bioactivity, or rate of bone bonding, of this dense glass exhibits a compositional dependency.[12] Kokubo and coworkers demonstrated that melt-derived glasses in the $CaO-SiO_2$ system show in vitro and in vivo bioactivity, with a maximum SiO_2 content of 65 mol %.[13−15] Since the beginning of the 1990s, sol−gel techniques have been applied to the processing of bioactive glasses.[16−31]

* Authors to whom correspondence should be addressed.
[†] Department of Chemistry.
[‡] Department of Chemical Engineering and Materials Science.

(1) Hench, L. L.; Splinter, R. J.; Allen, W. C.; Greenlee, T. K., Jr. *J. Biomed. Mater. Res.* **1971**, *2*, 117−141.
(2) Hench, L. L.; Wilson, J. *Introduction to Bioceramics*; World Scientific: Singapore, 1993.
(3) Hench, L. L. *J. Am. Ceram. Soc.* **1991**, *74*, 1487−1510.
(4) Hench, L. L. *J. Am. Ceram. Soc.* **1998**, *81*, 1705−1728.
(5) Kokubo, T. *A/W Glass-Ceramics: Processing and Properties*; World Scientific: Singapore, 1993.
(6) Kokubo, T.; Shigematsu, M.; Nagashima, Y.; Tashiro, M.; Yamamuro, T.; Higashi, S. *Bull. Inst. Chem. Res.* **1982**, *60*, 260−268.
(7) Wilson, J.; Pigott, G. H.; Schoen, F. J.; Hench, L. L. *J. Biomed. Mater. Res.* **1981**, *15*, 805.
(8) Wilson, J.; Nolletti, D. *CRC Handbook of Bioactive Ceramics: Bioactive Glasses and Glass-Ceramics*; Yamamuro, T., Hench, L. L., Wilson, J., Eds.; CRC Press: Boca Raton, FL, 1990; Vol. I., pp 283−302.
(9) Kokubo, T.; Kushitani, H.; Ohtsuki, C.; Sakka, S.; Yamamuro, T. *J. Mater. Sci.: Mater. Med.* **1992**, *3*, 79−83.
(10) Kokubo, T.; Kushitani, H.; Sakka, S.; Kitsugi, T.; Yamamuro, T. *J. Biomed. Mater. Res.* **1990**, *24*, 721−734.
(11) Kokubo, T. *CRC Handbook of Bioactive Ceramics; Bioactive Glasses and Glass-Ceramics*; Yamamuro, T., Hench, L. L., Wilson, J., Eds.; CRC Press: Boca Raton, 1990; Vol. I, pp 41−50.
(12) Ogino, M.; Ohuchi, F.; Hench, L. L. *J. Biomed. Mater. Res.* **1980**, *14*, 55−64.
(13) Ebisawa, Y.; Kokubo, T.; Ohura, K.; Yamamuro, T. *J. Mater. Sci.: Mater. Med.* **1990**, *1*, 239−244.
(14) Ohura, K.; Nakamura, T.; Yamamuro, T.; Kokubo, T.; Ebisawa, Y.; Kotoura, Y.; Oka, M. *J. Biomed. Mater. Res.* **1991**, *25*, 357−365.
(15) Ohtsuki, C.; Kokubo, T.; Yamamuro, T. *J. Non-Cryst. Solids* **1992**, *143*, 84−92.
(16) Jokinen, M.; Rahiala, H.; Rosenholm, J. B.; Peltola, T.; Kangasniemi, I. *J. Sol−Gel Sci. Technol.* **1998**, *12*, 159−167.
(17) Peltola, T.; Jokinen, M.; Rahiala, H.; Levanen, E.; Rosenholm, J. B.; Kangasniemi, I.; Yli-Urpo, A. *J. Biomed. Mater. Res.* **1999**, *44*, 12−21.
(18) Laczka, M.; Cholewa, K.; Mozgawa, W. *J. Mater. Sci. Lett.* **1995**, *14*, 1417−1420.
(19) Li, R.; Clark, A. E.; Hench, L. L. *J. Appl. Biomater.* **1991**, *2*, 231−239.
(20) Li, P.; Ohtsuki, C.; Kokubo, T.; Nakanishi, K.; Soga, N.; Nakamura, T.; Yamamuro, T. *J. Am. Ceram. Soc.* **1992**, *75*, 2094−2097.
(21) Li, P.; Nakanishi, K.; Kokubo, T.; de Groot, K. *Biomaterials* **1993**, *14*, 963−967.
(22) Li, R.; Clark, A. E.; Hench, L. L. *Chemical Processing of Advanced Materials*; Hench, L. L., West, J. K., Eds.; J. Wiley and Sons, Inc.: New York, 1992; p 627.
(23) Pereira, M. M.; Clark, A. E.; Hench, L. L. *J. Biomed. Mater. Res.* **1994**, *18*, 693−698.

10.1021/cm000895e CCC: $20.00
Published on Web 03/07/2001

Numerous in vitro studies of glasses in the CaO−P_2O_5−SiO_2, CaO−MgO−P_2O_5−SiO_2, and CaO−SiO_2 systems showed not only that the sol−gel method increases the HCA layer formation rate, but that it can also extend the SiO_2 content from 65 mol % in melt glasses to 90 mol %.[19,23] Some researchers reported that an HCA layer could even be formed on pure silica glasses obtained by a sol−gel method.[20,21,24,25,32,33] This enhanced bioactivity is associated with the surface charcteristics of sol−gel glasses, such as their high surface areas and porous textures. Although the influence of the surface structures on HCA formation is still not fully understood, several hypotheses have been suggested, on the basis of the effects of surface charge, texture (pore size and pore volume), and surface hydroxyl groups.[21,32,34−36] It is clear that the surface properties must play an important role in bioactivity, and if surface features can be enhanced through control of the sol−gel glass structure, one would expect further improvements of the bioactivity.

In the past few years, a novel technique, colloidal crystal templating, was reported to fabricate three-dimensionally ordered macroporous (3DOM) structures containing uniform pores with diameters of a few hundred nanometers.[37−39] By using close-packed arrays of monodisperse spheres [polystyrene, poly(methyl methacrylate) (PMMA), or silica] as templates, a large number of 3DOM materials have been prepared, including metal oxides, metals, alloys, polymers, and other compositions.[40] 3DOM structures have been investigated as photonic crystals, which exhibit interesting optical effects based on Bragg diffraction and the formation of photonic stopbands.[39,41,42] In addition, as porous supports, certain 3DOM structures can facilitate mass transport associated with heterogeneous chemical processes, such as catalysis, sorption, separation, and surface reactivity, because of their high accessible surface areas and bicontinuous networks of pores. In the present work, bioactive sol−gel glasses with and without 3DOM structures were prepared, and their in vitro activities toward HCA mineralization from SBF were compared. To obtain homogeneous structures and to simplify the data analysis, a $CaO{\cdot}4SiO_2$ binary system was chosen. To evaluate the mineralization of 3DOM glasses, a series of comparison studies were carried out by X-ray diffraction (XRD), Fourier transform infrared (FTIR) spectroscopy, scanning electron microscopy (SEM), transmission electron microscopy (TEM), N_2 adsorption, and chemical analysis.

Experimental Section

Preparation of 3DOM Glasses and Control Sample. Monodisperse PMMA spheres were synthesized and packed into colloidal crystals by gravitational settling.[40] The 3DOM glass was prepared by a sol−gel method as follows. $Ca(NO_3)_2{\cdot}4H_2O$ (4.72 g) was dissolved in 12 mL of 1 M HNO_3 solution. Tetraethyl orthosilicate (TEOS, 16.67 g) was added to the solution with vigorous stirring to obtain a nominal composition of 80 mol % SiO_2 and 20 mol % CaO. After 10−15 min of hydrolysis under stirring, a homogeneous sol was obtained. Stirring was stopped, and about 8 g of centimeter-scale, close-packed PMMA colloidal crystals were added to the solution. After 3−5 min of soaking, the impregnated colloidal crystals were transferred to a Büchner funnel, and suction was briefly applied to remove excess solution. These colloidal crystals were introduced into a sealed container, where the precursor was allowed to gel for 1 day at room temperature and was then aged for 1 day at 70 °C. Finally, the 3DOM glass was obtained by calcining the templated gel at the desired temperature (600−800 °C) in air for 1 h. All of the heating rates were 2 °C/min. For comparison, a control sample was prepared using the excess solution in the vacuum filtration stage by carrying out the same gelation, aging, and calcination processes (600 °C only), but without the colloidal crystal template. After grinding, the control sample consisted of coarse particles a few hundred micrometers in size.

Characterization. Suitable calcination temperatures for template removal and glass formation were determined by thermogravimetric analysis (TGA) and differential thermal analysis (DTA) of the dried templated gel. TGA was performed with a Perkin-Elmer TGA-7 thermogravimetric analyzer attached to a PC via a TAV7/DX thermal controller. DTA was performed with a Perkin-Elmer DTA 1700 instrument. Both thermal analyses were carried out from 25 to 1000 °C at 2 °C/min in air.

The glass samples were characterized by SEM and N_2 adsorption as described previously for 3DOM materials.[43] XRD patterns were obtained on a Bruker-AXS microdiffractometer with a 2.2-kW sealed Cu X-ray source. Chemical analyses for carbon and hydrogen were carried out at Atlantic Microlab, Inc., Norcross, GA. ^{29}Si MAS NMR spectra (single-pulse) were obtained on a Chemagnetics CMX-400 Infinity spectrometer at room temperature with a 7.5-mm zirconia rotor spinning at

(24) Pereira, M. M.; Clark, A. E.; Hench, L. L. *J. Am. Ceram. Soc.* **1995**, *78*, 2463−2468.
(25) Pereira, M. M. *J. Sol−Gel Sci. Technol.* **1996**, *7*, 59−68.
(26) Izquierdo-Barba, I.; Salilnas, A. J.; Vallet-Regí, M. *J. Biomed. Mater. Res.* **2000**, *51*, 191−199.
(27) Izquierdo-Barba, I.; Salilnas, A. J.; Vallet-Regí, M. *J. Biomed. Mater. Res.* **1999**, *47*, 243−250.
(28) Pérez-Pariente, J.; Balas, F.; Roman, J.; Salilnas, A. J.; Vallet-Regí, M. *J. Biomed. Mater. Res.* **1999**, *47*, 170−175.
(29) Vallet-Regí, M.; Romero, A. M.; Ragel, C. V.; LeGeros, R. Z. *J. Biomed. Mater. Res.* **1998**, *44*, 416−421.
(30) Vallet-Regí, M.; Salinas, A. J.; Román, J.; Gil, M. *J. Mater. Chem.* **1999**, *9*, 515−518.
(31) Vallet-Regí, M.; Acros, D.; Pérez-Pariente, J. *J. Biomed. Mater. Res.* **2000**, *51*, 23−28.
(32) Li, P.; Ohtsuki, C.; Kokubo, T.; Nakanish, K.; Soga, N.; Nakamura, T.; Yamamuro, T. *Mater. Med.* **1993**, *4*, 127−131.
(33) Li, P.; Ohtsuki, T.; Kokubo, T.; Nakanish, K.; Soga, N.; Nakamura, T.; Yamamuro, T. *J. Appl. Biomater.* **1993**, *4*, 221−229.
(34) Li, P.; Zhang, F. *J. Non-Cryst. Solids.* **1990**, *119*, 112.
(35) Li, P.; de Groot, K. *J. Biomed. Mater. Res.* **1993**, *27*, 1495.
(36) Li, P.; Ohtsuki, C.; Kokubo, T.; Nakanish, K.; Soga, N.; de Groot, K. *J. Biomed. Mater. Res.* **1994**, *28*, 7.
(37) Velev, O. D.; Jede, T. A.; Lobo, R. F.; Lenhoff, A. M. *Nature* **1997**, *389*, 447−448.
(38) Holland, B. T.; Blanford, C. F.; Stein, A. *Science* **1998**, *281*, 538−540.
(39) Wijnhoven, J. E. G. J.; Vos, W. L. *Science* **1998**, *281*, 802−804.
(40) Yan, H.; Blanford, C. F.; Smyrl, W. H.; Stein, A. *Chem. Commun.* **2000**, *16*, 1477−1478 and references therein.
(41) Thijssen, M. S.; Sprik, R.; Wijnhoven, J. E. G. J.; Megens, M.; Narayanan, T.; Lagendijk, A.; Vos, W. L. *Phys. Rev. Lett.* **1999**, *83*, 2730−2733.
(42) Blanco, A.; Chomski, E.; Grabtchak, S.; Ibisate, M.; John, S.; Leonard, S. W.; Lopez, C.; Meseguer, F.; Miguez, H.; Mondia, J. P.; Ozin, G. A.; Toader, O.; Driel, H. M. *Nature* **2000**, *405*, 437−440.
(43) Yan, H.; Blanford, C. F.; Holland, B. T.; Smyrl, W. H.; Stein, A. *Chem. Mater.* **2000**, *12*, 1134−1141.

4 kHz (79.4 MHz, pulse width = 3 μs, pulse delay = 40 s).

Evaluation of Mineralization from SBF. The in vitro activity toward mineralization was evaluated by soaking certain amounts of samples (5, 10, 20, and 50 mg) in 50 mL of SBF (142.0 mM Na^+, 5.0 mM K^+, 2.5 mM Ca^{2+}, 1.5 mM Mg^{2+}, 148.8 mM Cl^-, 4.2 mM HCO_3^-, and 1.0 mM HPO_4^{2-})[9] in polypropylene bottles maintained at 37 °C. After chosen reaction times, the SBF was sampled, and the solids were separated by vacuum filtration, washed three times with methanol, and dried in air. A model 215 pH meter (Denver Instrument) was used to measure the pH value of the SBF. The concentrations of Si, P, and Ca in the SBF were analyzed by inductively coupled plasma (ICP) atomic emission spectroscopy (AES) by the Geochemical Lab, University of Minnesota, Minneapolis, MN. The dried glass samples were studied by FTIR spectroscopy, XRD, SEM, and TEM. FTIR spectra were acquired on a Nicolet Magna FT-IR 760 spectrometer. The pellets for FTIR experiments were prepared by mixing the dried samples with KBr powder. Samples for TEM were prepared by sonicating about 5 mg of the powder in 2 mL of absolute ethanol for 2 min and then depositing five drops of the suspension on a holey carbon grid. TEM images were obtained with a Philips CM30 TEM instrument operating at 300 kV with a LaB_6 filament; images were recorded on a CCD.

Results and Discussion

Thermal Analysis. Judging from the TGA and DTA curves, the dried composite consisting of the inorganic gel within the PMMA colloidal crystal template loses ca. 8% mass between room temperature and ca. 230 °C, through elimination of residual water and alcohol in the sample. A more rapid weight loss of 79% occurs from 230 to 450 °C, which is associated with the removal of the PMMA template, as well as the elimination of nitrate decomposition products. The DTA curve exhibits an endothermic peak at 290 °C, due to the decomposition of the polymer template, which is followed by an exothermic peak at 363 °C associated mostly with the combustion of the polymer. The latter peak is superimposed on a continuing endothermic background related to the decomposition of nitrate. In the temperature range from 450 to 1000 °C, the weight remains almost constant, and no obvious endothermic or exothermic peaks are observed. These results allowed us to determine that the minimum temperature to obtain the template-free glass is ca. 450 °C. In this study, three temperature points, i.e., 600, 700, and 800 °C, were chosen to investigate the effect of the calcination temperature on the in vitro bioactivity of the glass, and the samples were labeled 3DOM600, 3DOM700, and 3DOM800, respectively.

Characterization of the 3DOM Glass. After calcination at 600 °C or higher, the template-free samples consisted of millimeter-scale particles that showed opalescence in multiple colors. Carbon and hydrogen analyses of the samples (Table 1) indicated that the PMMA templates and ethoxide groups were nearly completely removed during calcination. Figure 1 shows a typical SEM image of the 3DOM600 sample. Uniform voids surrounded by inorganic walls formed an ordered macroporous structure, in which the array of voids exhibited an fcc arrangement.[44] The Fourier transform of the image (inset in Figure 1) showed several orders of spots, confirming the long-range periodicity of the macropore structure. With 470-nm PMMA spheres as templates, average pore diameters of 410 nm were obtained. The macropores were interconnected in three dimensions through windows whose diameters typically exceeded 100 nm. This bicontinuous network of voids and solid skeleton permitted free infiltration of liquids. Judging from the SEM images, the 3DOM glass walls had a typical thickness of 30 nm. No diffraction peaks were observed in the XRD pattern except for a broad band between 20° and 35° 2θ, suggesting that, at this stage, the walls were amorphous.

Table 1. Textural Properties of 3DOM Glass and Control Sample Treated at the Indicated Temperatures and Corresponding Chemical Analysis Data

	temp (°C)	surface area (m^2/g)	pore volume[a] (mL/g)	chemical analysis C (wt %)	chemical analysis H (wt %)
3DOM glass	600	45.2	0.11	0.52	0.88
	700	44.2	0.12	0.32	0.77
	800	44.4	0.09	0.13	0.00
control sample	600	234	0.30	N/A	

[a] Does not include the macropore volume.

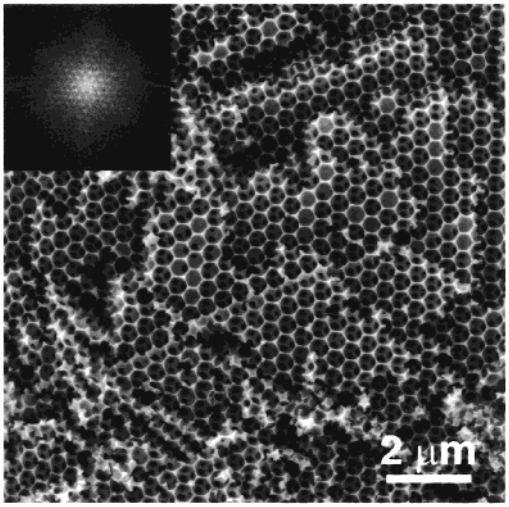

Figure 1. SEM image of 3DOM $CaO{\cdot}4SiO_2$ calcined at 600 °C (3DOM600) and corresponding Fourier transform of the image (inset).

The texture of the wall was studied by nitrogen adsorption measurements. Figure 2 shows the N_2 adsorption isotherms of 3DOM600 and a nontemplated control sample prepared at 600 °C. A type-II nitrogen adsorption isotherm was observed for the 3DOM600 sample, typical for a nonporous or macroporous adsorbent with no significant mesoporosity.[45] The BET (Brunauer−Emmett−Teller) specific surface areas of the 3DOM glasses prepared at varying temperatures are listed in Table 1. The surface area of 3DOM600 is 45.2 m^2/g. This value remains basically unchanged with increasing calcination temperature from 600 to 800 °C.

(44) Holland, B. T.; Blanford, C. F.; Do, T.; Stein, A. *Chem. Mater.* **1999**, *11*, 795−805.
(45) Sing, K. S. W.; Everett, D. H.; Haul, R. A. W.; Moscou, L.; Pierotti, R. A.; Rouquerol, J.; Siemieniewska, T. *Pure Appl. Chem.* **1985**, *57*, 603−619.

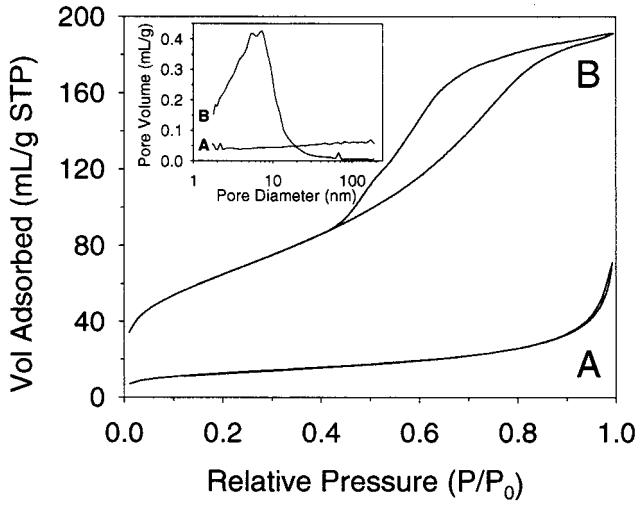

Figure 2. Nitrogen adsorption/desorption isotherms and BJH pore size distributions of (A) 3DOM600 and (B) a nontemplated control sample calcined at 600 °C.

The isotherm for the control sample, which was prepared without PMMA templates, is of type IV, indicating the presence of mesopores. The pore volume plot for this sample reveals a broad distribution of mesopores with diameters from 2 to 30 nm. These mesopores give rise to a higher surface area of 234 m^2/g.

The difference in mesopore structure for the templated and nontemplated sol−gel glasses is related to the additional macroporosity in the 3DOM materials. During the heating process, shrinkage occurs, and the gel network densifies because of continued condensation of internal silanol groups, structural relaxation, and capillary strain.[46] All of these processes depend on material transport, such as elimination of solvent, water, and alkoxide groups. In the 3DOM glass, such transport is greatly facilitated by the large voids, as well as by the relatively thin walls. Excess free volume due to mesoporosity in the gel is therefore more easily removed, leading to the lower mesopore volume and surface areas in the 3DOM materials.

Effect of the Bioactive Solid/SBF Ratio on Activity toward Mineralization. In an in vivo examination of bioactive materials, the concentration of inorganic ions in blood plasma remains relatively constant because of continual replenishment of fresh blood plasma, although this might not necessarily be the case close to an implant surface. Continuous flow of body fluids has been modeled in previous in vitro tests of bioactive sol−gel glasses.[26] In the present experiments, we employed more commonly used static tests to examine the propensity of 3DOM glasses for apatite formation; such tests have been correlated with the in vivo bone-bonding ability of bioactive materials.[10,11] Because of the limited amount of ions available for apatite growth in these tests, the ratio of bioactive solid to SBF is important. At lower ratios, the changes in ion concentration are minimized, giving a better approximation of in vivo conditions. The effects of variations in this ratio are discussed in this section.

To investigate these effects, 3DOM600 samples were soaked in SBF at solid/SBF ratios of 0.1, 0.2, 0.4, and 1.0 mg/mL. Figure 3 shows the FTIR spectra of these samples after 3 days of soaking. The absorption bands at 1080, 800, and 470 cm^{-1} correspond to the asymmetric Si−O−Si stretch, the symmetric Si−O−Si stretch, and the Si−O−Si deformation mode, respectively. No nitrate absorptions are present, indicating that, at 600 °C, all nitrate had been removed from the templated sample (see also Figure 4A, untreated). Absorptions due to phosphate and carbonate groups can be observed in the spectra of all samples, suggesting that deposition of amorphous calcium phosphate and/or HCA occurred (carbonate and hydroxide might also be present in the amorphous phase, but it will be called calcium phosphate in this paper). For the 0.4 and 1.0 mg/mL samples, the phosphate group shows a low intensity band at 567 cm^{-1}, which corresponds to the antisymmetric vibrational mode of P−O in amorphous calcium phosphate. For the 0.1 and 0.2 mg/mL samples, the bands of the phosphate group at 1034, 962, 603, and 562 cm^{-1}, together with the bands of the carbonate group at 1488, 1432, and 873 cm^{-1}, can be assigned to the crystalline HCA. It is notable that, for larger proportions of 3DOM glass, the relative intensity of the phosphate absorption band at 567 cm^{-1} decreased, while the relative intensity of the silicate band at 470 cm^{-1} increased. In addition, the FTIR spectra indicate that the structure of the precipitate was amorphous calcium phosphate at higher loadings of the 3DOM solid and became more crystalline HCA for lower loadings.

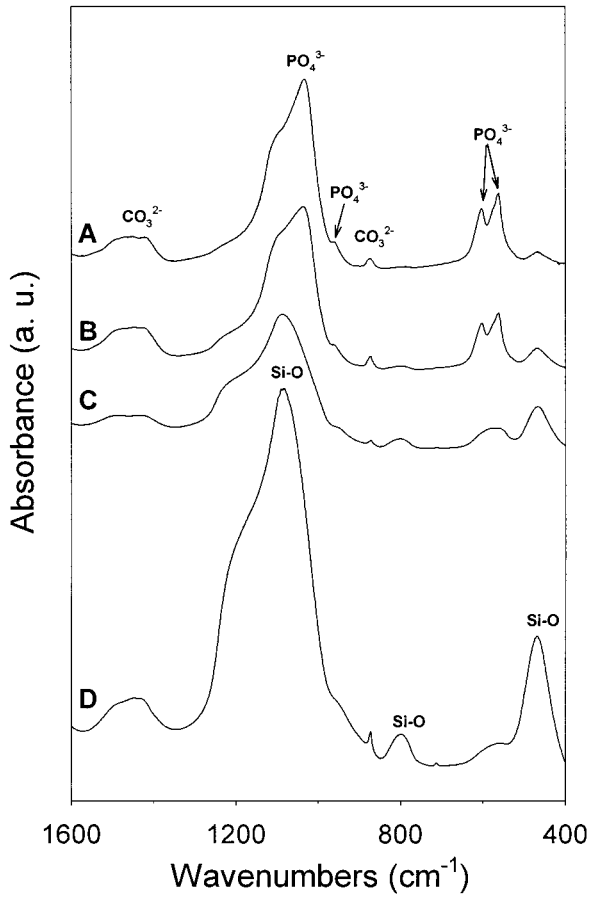

Figure 3. FTIR spectra of 3DOM600 soaked in SBF for 3 days, using the following ratios of 3DOM600/SBF. (A) 0.1, (B), 0.2, (C) 0.4, and (D) 1.0 mg/mL.

(46) Brinker, C. J.; Scherer, G. W. *Sol−Gel Science*; Academic Press: Boston, MA, 1990.

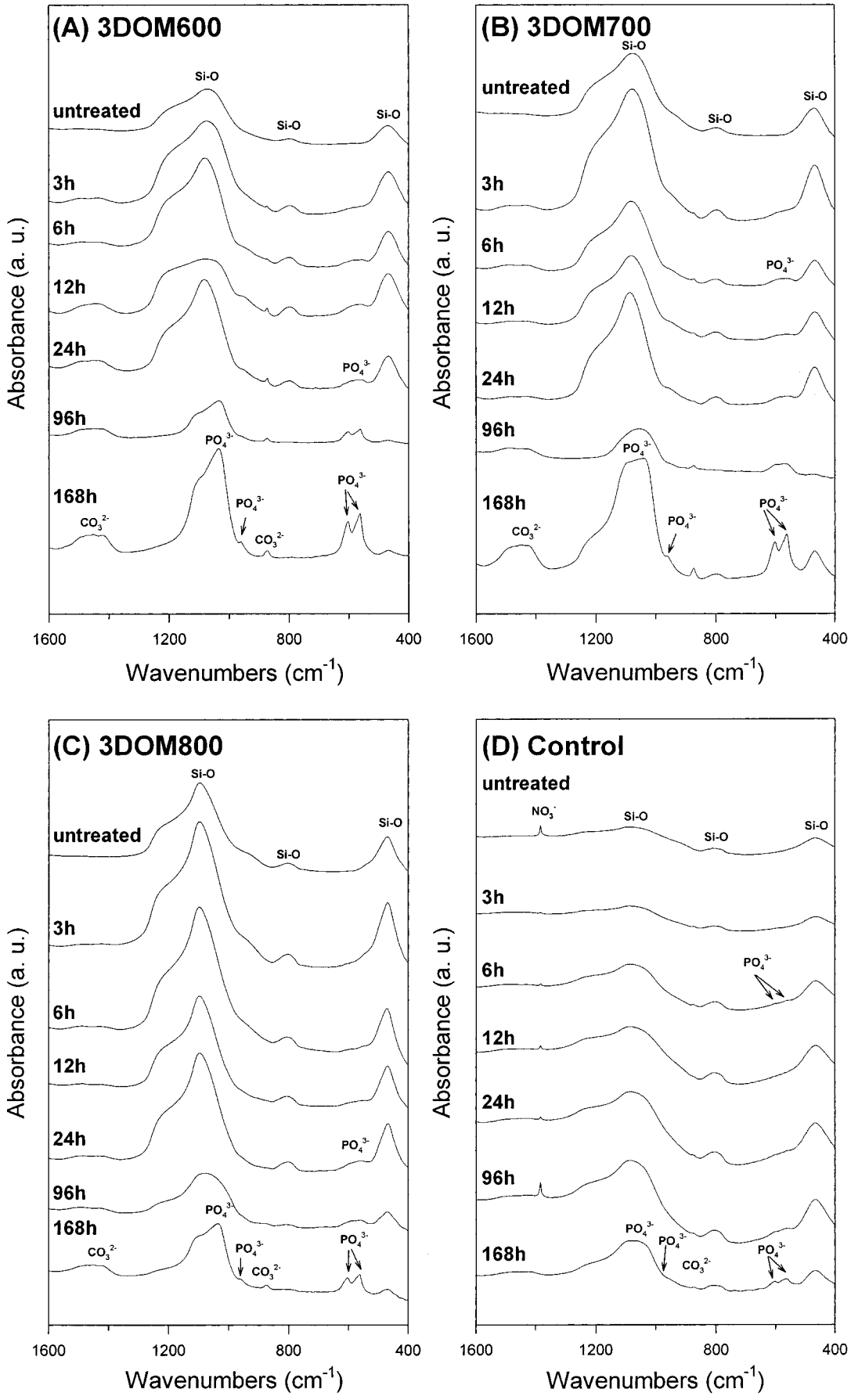

Figure 4. FTIR spectra of 3DOM $CaO{\cdot}4SiO_2$ calcined at (A) 600 °C (3DOM600), (B) 700 °C (3DOM700), and (C) 800 °C (3DOM800) and (D) a nontemplated control sample calcined at 600 °C as prepared and after immersion of the solid samples in SBF (0.1 mg/mL) for the indicated lengths of time.

On the basis of the known mechanism for the formation of apatite, these observations can be explained as follows. In bioactive silica-based glasses, a layer of high-surface-area silica gel is first formed by partial network dissolution and surface polycondensation.[3,4] It has been suggested that this silica gel plays a significant role in HCA formation because the silanol groups present on the surface provide deposition sites for calcium phosphate from a metastable calcium phosphate solution (i.e., the SBF).[19,20] The number of possible deposition sites increases with the amount of bioactive sol−gel glass present, the surface area, and the reactivity of the surface (number of accessible surface Si−OH groups). Amorphous calcium phosphate, initially formed, crystallizes into an HCA phase analogous to that present in bone. According to studies by LeGeros et al.[47] and Izquierdo-Barba et al.,[27] this HCA phase has crystallite sizes less than 150 Å and appears amorphous by XRD and FTIR spectroscopy. The HCA nanocrystallites can continue to grow and form a crystalline structure that is detectable by XRD and FTIR spectroscopy if the SBF can provide more HPO_4^{2-} and Ca^{2+} and the SBF and the glass can provide more Ca^{2+}, as long as a critical concentration of HCA precipitate is maintained. In the extreme case (low ratio of phosphate to silicate), if too many deposition sites are present in the system and many of the Ca^{2+} or HPO_4^{2-} ions are consumed for the precipitation of calcium phosphate and HCA nanocrystallites, the growth of HCA is impeded, and only an amorphous phase can be produced.

Evaluation of the HCA Mineralization of the 3DOM Glass. To evaluate the in vitro bioactivity of the 3DOM glass, the formation of HCA as a function of soaking time in SBF was investigated in FTIR, ICP, XRD, and SEM experiments. Figure 4A shows the FTIR spectra of 3DOM600 before soaking and after 3, 6, and 12 h, and 1, 4, and 7 days in SBF at body temperature. A standard loading of 0.1 mg/mL of 3DOM glass in SBF was chosen, a ratio that leads to an HCA product, as noted above. For comparison, the FTIR spectra of a nontemplated control sample soaked in SBF (0.1 mg/mL) are also shown in Figure 4D.

After 3DOM600 was soaked for 3 h in SBF, a weak shoulder appeared in the P−O bending region at 567 cm^{-1}, indicating the presence of phosphate on the glass. After 6 h, this band was well resolved and displayed the shape typical for amorphous phosphate.[27] SEM data corroborated the FTIR results. A high-magnification SEM image of the untreated 3DOM solid reveals that the skeletal surface is continuous and relatively smooth before soaking (Figure 5A). After treatment in SBF for 3 h, small spheres completely cover the surface of the wall (Figure 5B). Most of the spheres have diameters of less than 50 nm. Because the XRD pattern shows no crystalline features at this stage, it can be concluded that the spheres consist of amorphous calcium phosphate or HCA nanocrystallites.

After 4 days of soaking, absorptions characteristic for crystalline HCA appeared at 603 and 562 cm^{-1} in the FTIR spectrum. The intensity of this doublet increased with further soaking time. The SEM shows a typical morphology of HCA in the 4-day sample (Figure 5C).

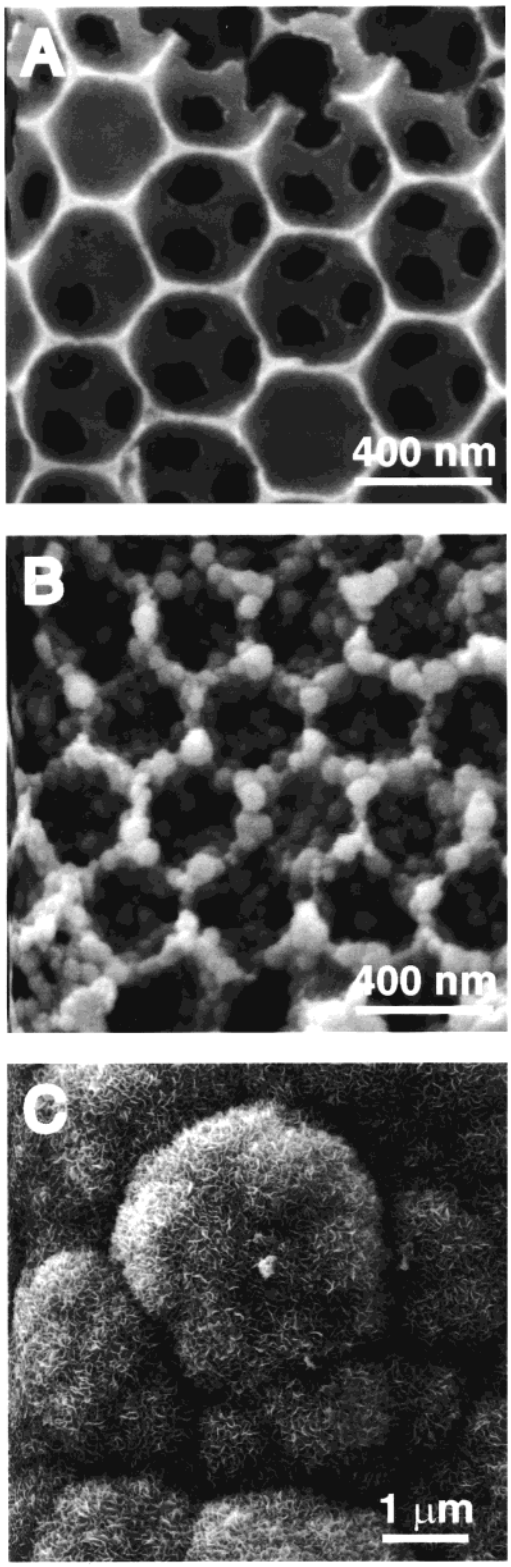

Figure 5. SEM images of (A) 3DOM600, (B) the same sample after immersion in SBF (0.1 mg/mL) for 3 h, and (C) the same sample after immersion in SBF for 4 days.

Numerous uniform flakelike crystallites form spherical aggregates that are several micrometers in diameter. The XRD pattern of the sample shows four peaks, which match the diffraction pattern of hydroxyapatite (JCPDS 9-432).

A comparison with infrared data for a nontemplated control sample revealed several differences from the

(47) LeGeros, J. P.; Trautz, O. R.; LeGeros, R. Z. *Trans. Am. Cryst. Assn.* **1965**, 40.

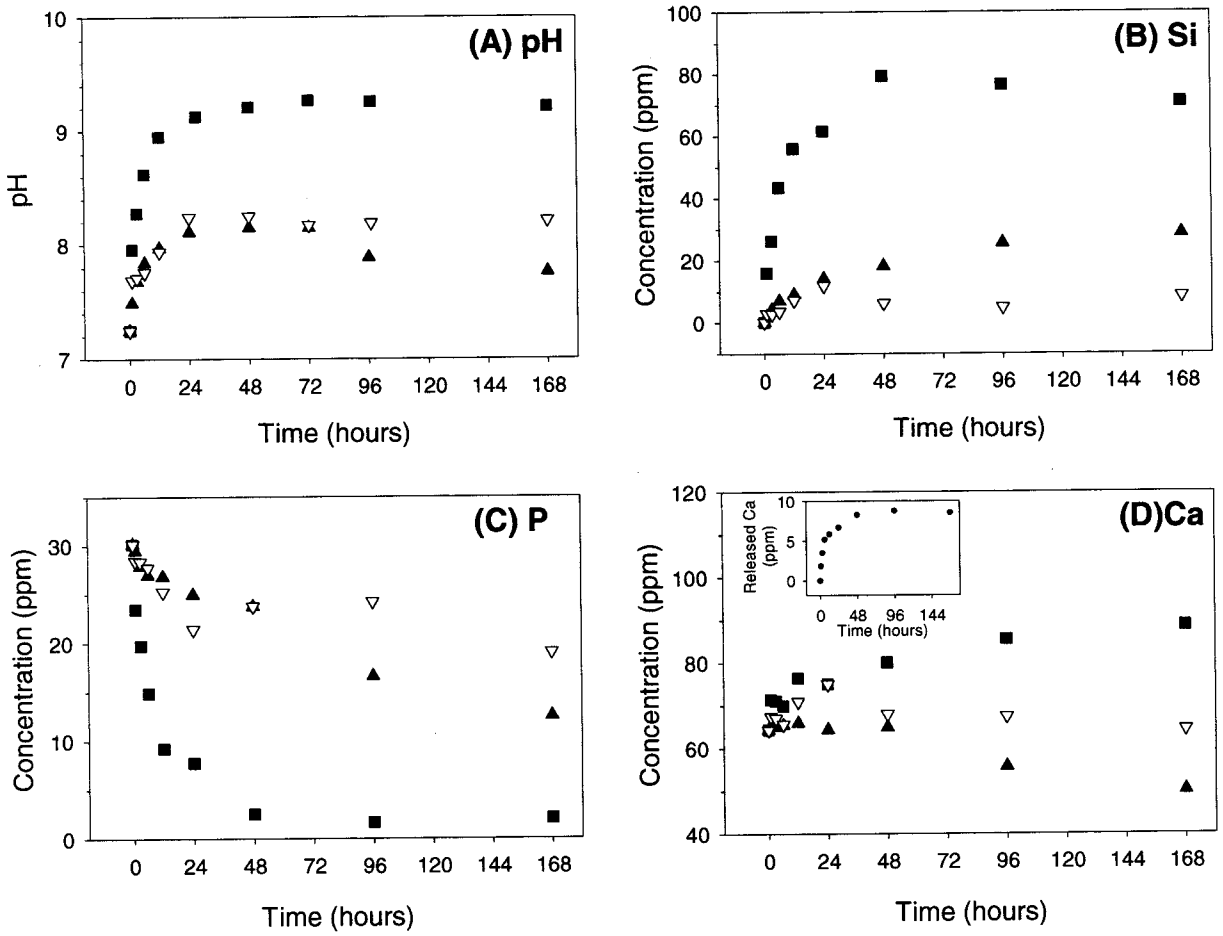

Figure 6. Variations of (A) pH and (B) Si, (C) P, and (D) Ca concentrations in SBF with time for 3DOM600 (▲, 0.1 mg/mL; ■, 1.0 mg/mL), and control sample (▽, 1.0 mg/mL) in SBF. The inset in part D shows the change in Ca concentration derived from the 3DOM600 sample (0.1 mg/mL) (difference between total Ca and P concentration plots).

3DOM material. The FTIR spectrum of the control sample exhibited an absorption at 1384 cm^{-1} that can be assigned to a stretching vibration of the nitrate group, indicative of residual NO_3^- in the glass network. It has been shown that calcination above 700 °C is required to remove all nitrate from a nontemplated $CaO{\cdot}4SiO_2$ glass.[48] After 6 h of soaking, two very weak FTIR absorptions appeared at 603 and 562 cm^{-1}, which might correspond to crystalline HCA. These bands remained weak up to 7 days of soaking, when fully developed phosphate and carbonate absorptions were seen. Even after this time, these absorptions were less intense relative to the silica absorptions than the corresponding peaks in the 3DOM samples. This behavior is different from a previously reported result,[27] where an induction time of 3 h for HCA growth and a larger intensity ratio of phosphate absorptions to silicate absorptions after 7 days were observed for a glass with the same composition. We speculate that the discrepancy might be due to different sampling techniques for the FTIR analysis. In the study of Izquierdo-Barba et al.,[27] a glass disk (13 mm in diameter, 2 mm in height, and 0.5 g in weight) was soaked in 50 mL of SBF for a desired time; then, the pellets for FTIR were prepared by mixing materials scraped from the glass surface with KBr. In our study, the pellets for FTIR were prepared by mixing the treated glass with KBr directly. Therefore, our FTIR results represent an average "bulk" property, whereas the previous study would emphasize surface compositions.

Figure 6 shows the variations of pH and Si, P, and Ca concentrations as functions of the soaking time for 3DOM600 in SBF at ratios of 0.1 and 1 mg/mL. The data for the 1 mg/mL control sample in SBF are also included for comparison. The pH changes are determined by the chemical reactions in SBF associated with the formation of phosphate and HCA. In the $CaO-SiO_2$ glass, two main reactions influence the pH. One reaction is the interchange between Ca^{2+} from the substrate and protons from the solution, which results in an increase in the pH value.[4,28,49] Another reaction involves the hydrolysis and dissolution of silica, which decreases the pH value.[50] This reaction is favored when the pH value increases. The actual pH depends on the competition between these two reactions. For the 0.1 mg/mL sample, it can be seen that the Ca^{2+} concentration in solution remained almost constant for 2 days of soaking and then slowly decreased (Figure 6D). The Ca^{2+} concentration is controlled by both the release of Ca^{2+} from the substrate and the formation of phosphate or HCA. Ca^{2+} consumption associated with HCA formation correlates with the depletion of P from solution. The difference between the Ca^{2+} and P concentration plots (Figure 6C

(48) Hayashi, T.; Saito, H. *J. Mater. Sci.* **1980**, *15*, 1971−1977.

(49) Kokubo, T. *An. Quim. Int. Ed.* **1997**, *93*, S49−S55.

(50) Unger, K. K. *J. Chromatogr. Libr.* **1979**, *16*, 1−14.

and 6D), i.e., the amount of Ca^{2+} released from the glass (Figure 6D, inset), indicate that the release rate of Ca^{2+} progressively decreased with soaking time. On the other hand, the Si concentration continued to increase as a function of the soaking time. Because the pH value depends on both of these concentrations, it started to decrease after 3 days for the 0.1 mg/mL sample. For the 1.0 mg/mL 3DOM600 sample, after a significant increase in the first 2 days, the Si concentration remained almost constant at 80 ppm, suggesting saturation. Simultaneously, after experiencing a large drop from 30 to 2.5 ppm, the P concentration did not change any more, indicating the termination of HCA formation. Combined with the slow increase of the Ca^{2+} concentration, this pattern explains the constant pH curve for the 1 mg/L sample after 2 days.

It should be noted that, in comparison to the results for the 3DOM glass, none of the Si, P, or Ca concentrations changed significantly for the control sample, even though a larger loading amount of control sample was used (1.0 mg/mL) and the control sample exhibited a higher specific surface area (234 m^2/g). This behavior indicates that the control exhibits a lower chemical reactivity, in agreement with the FTIR results. Judging from the residual P and Ca concentrations in SBF, the lower reactivity of the control sample cannot be explained by depletion of these species, an effect that would prevent HCA growth. Because the 3DOM glass and the control had the same chemical composition, the difference in reactivity is likely due to the different pore and surface structures. As the N_2 adsorption measurements revealed, the control contained a distribution of mesopores with an average diameter of 5.1 nm. Although the surface area of the control sample was very high, a large fraction of the internal surface might not have been readily accessible to the SBF solution because of diffusion limitations and deposition of HCA in the pores at the surface. For the 3DOM sample, on the other hand, the material had a higher void fraction (ca. twice that of the control) and macropores that were several hundred nanometers in diameter. In addition, the ordered array of 3D interconnected macropores minimized traps or dead spots. These factors allowed the SBF to infiltrate the material freely and permitted more efficient transport of ions to and from the reactive surface, resulting in the better activity of the 3DOM glasses toward mineralization.

Effect of Calcination Temperature. Figure 4B and 4C shows the FTIR spectra of 3DOM700 and 3DOM800, respectively, before and after soaking in SBF as a function of the soaking time. For 3DOM700, the behavior paralleled that for 3DOM600 during the first 24 h, showing an envelope associated with amorphous phosphate around 567 cm^{-1}. After 4 days, a doublet at 603 and 562 cm^{-1} was seen, but it was much less resolved than in the 3DOM600 sample, indicating that the transition from amorphous calcium phosphate to crystalline HCA was delayed after higher-temperature calcination. After 7 days of soaking, crystallization had progressed significantly, as indicated by a well-resolved phosphate doublet. For 3DOM800, the induction time for the formation of an amorphous phosphate layer increased to 12 h, longer than for the samples calcined at lower temperatures. In addition, even after 4 days of soaking, the precipitate was still predominantly amorphous calcium phosphate. The doublet bands of crystalline HCA at 603 and 562 cm^{-1} could be observed only after 7 days of soaking. These results indicate that the activity of the 3DOM glass decreases with calcination temperature.

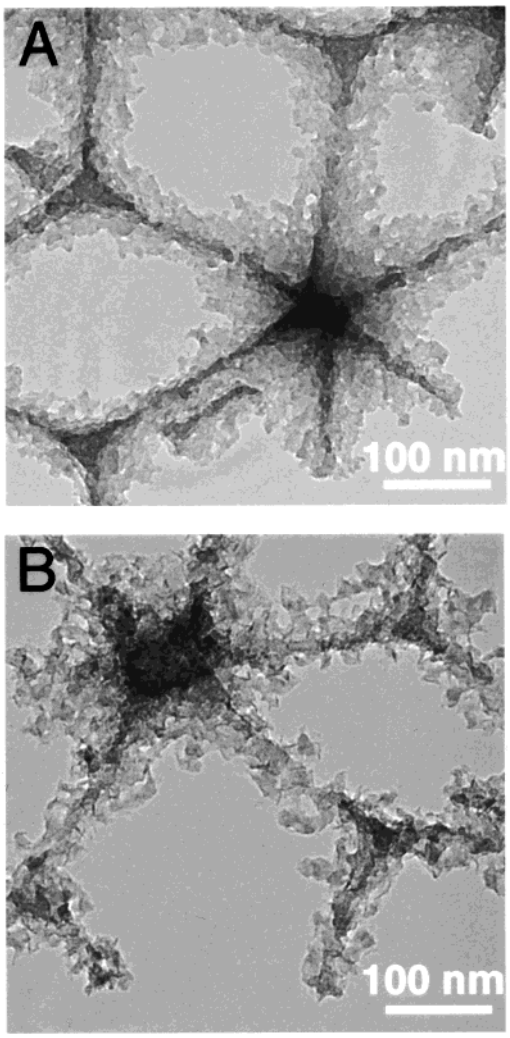

Figure 7. TEM images of 3DOM600 after (A) 1 day and (B) 7 days of immersion in SBF (1.0 mg/mL).

This tendency is in agreement with results reported for nontemplated bioactive glasses by other investigators.[32,51] They attributed the effect of calcination temperature on bioactivity to changes in the physical characteristics of the surface (surface area, pore size) or the surface chemistry (hydroxyl groups). For the present materials, the effect is more likely due to the influence of hydroxyl groups (greater degree of condensation at higher temperature), because all three 3DOM samples calcined between 600 and 800 °C had almost the same textural properties but a decreasing hydrogen content. In addition, ^{29}Si solid-state NMR experiments showed that the intensity ratio of the Q^3 ([Si*$(OSi)_3$-OH] to Q^4 [Si*$(OSi)_4$] resonances decreased significantly from the 3DOM600 to the 3DOM800 sample, comfirming the loss of the silanol group upon higher-temperature calcination.

(51) Hench, L. L.; Wang, S. H.; Nogues, J. L. *Multifunctional Materials*; Gunshor, R. L., Ed.; SPIE: Bellingham, WA, 1988; p 76.

Dissolution Characteristics of the 3DOM Glass. The 3DOM glass shows rapid dissolution behavior, which is expressed in faster release of Si compared to the control sample. According to the ICP results, when 3DOM600 was soaked in SBF (1.0 mg/mL), the Si concentration in the liquid rose from 0 to 61.6 ppm after 1 day, which amounts to 16.3% of Si in the substrate. After 2 days of soaking, the Si concentration appeared to reach a saturation point and remained constant at about 80 ppm, corresponding to 21.1% of the Si. Figure 7 shows the TEM micrographs of 3DOM600 after being soaked in SBF (1.0 mg/mL) for 1 and 7 days, respectively. Because of etching with SBF, the wall structure of the 7-day sample was thinner and showed more textural porosity than that of the 1-day sample. In some areas, particles were only tenuously connected. For a lower ratio of 3DOM600 in SBF (0.1 mg/mL), the Si concentration increased steadily from 0 to 28.5 ppm after 7 days, which amounted to 75.3% of the Si in the substrate. As a result, all of the walls collapsed, and 3DOM structures could not be observed by SEM (Figure 5C). In comparison, the control sample dissolved much more slowly. After the control was soaked in SBF (1.0 mg/mL) for 7 days, only 3% of the Si was released. The high release rate of Si in 3DOM glass is closely related to its macroporous structure, in particular, its highly accessible surface and thin wall structure.

The dissolution character is an important parameter that should be considered in applications involving biological implant materials. In some applications (e.g., bone fillers), the rapid dissolution of the filler coincident with replacement by bony tissue is desired. The dissolution rate of the 3DOM glass is fast and, if desired, can be modified by varying the thermal history or the composition of the material. Judging from the present investigations, these qualities make 3DOM glasses promising materials for some biological applications.

Conclusions

Colloidal crystal templating is a general method that can be applied to generate 3DOM structures with a large number of compositions. This study focuses on the $CaO{\cdot}4SiO_2$ system, but other binary, ternary, or higher bioactive glass compositions should also be feasible and might lead to further improvements in bioactivity. 3DOM glasses exhibit several features relevant for bioactive materials that result in their faster dissolution and more rapid growth of HCA in SBF. These features include (1) the size of the overall 3DOM particle (up to millimeter-size), which should prevent rejection of the particle by the body defense system; (2) the large pores, which permit facile transport of SBF and probably also natural body fluids; (3) the thin walls, which are generated by filling interstices between close-packed templating spheres; and (4) the relatively large accessible surface. Comparisons with a nontemplated control sample indicate that the relevant surface is not that which is accessible to small gas molecules, such as nitrogen molecules typically used in gas sorption measurements, but that which can be easily reached by more viscous fluids containing solvent and multiple ions. The study showed that, in a limited SBF supply, HCA formation was favored by smaller 3DOM solid/SBF ratios that reduced the number of deposition sites for calcium phosphate formation and increased the yield of HCA. Similar to nontemplated bioactive glasses, the in vitro activity of the 3DOM glasses toward mineralization depended on their thermal history and decreased with higher calcination temperatures in the range from 600 to 800 °C, thereby providing some tunability of the reactivity according to the requirements of specific applications.

Acknowledgment. We thank 3M, Dupont, the David and Lucile Packard Foundation, the McKnight Foundation, the National Science Foundation (DMR-9701507) and the MRSEC Program of the NSF (DMR-9809364) for support of this research.

Supporting Information Available: TGA and DTA curves of the colloidal crystal-templated $CaO{-}SiO_2$ gel still containing PMMA spheres. XRD patterns of 3DOM600, the same sample after immersion into SBF (0.1 mg/mL) for 3 h, and the same sample after immersion for 3 days. This material is available free of charge via the Internet at http://pubs.acs.org.

CM000895E